



Published in final edited form as:

J Autoimmun. 2010 March ; 34(2): 96. doi:10.1016/j.jaut.2009.07.003.

Roles for Catharsis S, L, and B in Insulinitis and Diabetes in the NOD Mouse

Lianne C. Hsing¹, Elizabeth A. Kirk², Timothy S. McMillen³, Shuo-Hung Hsiao³, Mark Caldwell³, Barbara Houston³, Alexander Y. Rudensky⁴, and Renee C. LeBoeuf³

¹Department of Immunology and Howard Hughes Medical Institute, University of Washington, Seattle, WA

²Nutritional Sciences Interdisciplinary Program, School of Public Health and Community Medicine, University of Washington, Seattle, WA

³Department of Medicine, Division of Metabolism, Endocrinology and Nutrition, University of Washington, Seattle, WA

⁴Department of Immunology, Memorial Sloan-Kettering Cancer Center, New York, NY

Abstract

We developed a panel of non-obese diabetic (NOD) mice deficient in major lysosomal cysteine proteases (cathepsins S, L and B) to identify protease enzymes essential for autoimmune diabetes. Null alleles for cathepsins (Cts) S, L or B were introgressed onto the NOD genetic background with 19 *Idd* markers at homozygosity. Diabetes onset was determined among females aged up to 6 months. We evaluated insulinitis and sialadenitis in tissues using histology and computer assisted morphology. NOD mice deficient in *Ctss* or *Ctsb* were partially protected from diabetes with incidence at 33% and 28%, respectively, versus wild-type NOD (69%; $p < 0.00001$). NODs lacking cathepsin L (*Ctsl* $-/-$) are completely protected from IDDM, as originally shown by others. *Ctsl*, *Ctss*, or *Ctsb* heterozygous mice were able to develop IDDM, although incidence levels were significantly lower for *Ctsb* $+/-$ (50%) and *Ctsl* $+/-$ (55%) as compared to NODs (69%; $p < 0.03$). *Ctsl* $-/-$ mice contain functional, diabetogenic T-cells and an enriched Foxp3⁺ regulatory T-cell population, and diabetes resistance was due to the presence of an expanded population of regulatory T-cells. These data provide additional information about the potency of the diabetogenic T-cell population in *Ctsl* $-/-$ mice which were comparable in potency to wild-type NOD mice. These data illustrate the critical contribution of each of these proteases in determining IDDM in the NOD mouse and provide a useful set of models for further studies.

Keywords

cathepsin; type 1 diabetes; mouse; NOD

Correspondence to: Renée C. LeBoeuf, Ph.D., Research Professor, Division of Metabolism, Endocrinology and Nutrition, Department of Medicine, 315 Mercer Street, Box 358050, University of Washington, Seattle, WA 98109-8050, Tele: +1 206-543-5208, FAX: +1 206-685-3662, leboeuf@u.washington.edu.

Publisher's Disclaimer: This is a PDF file of an unedited manuscript that has been accepted for publication. As a service to our customers we are providing this early version of the manuscript. The manuscript will undergo copyediting, typesetting, and review of the resulting proof before it is published in its final citable form. Please note that during the production process errors may be discovered which could affect the content, and all legal disclaimers that apply to the journal pertain.

INTRODUCTION

The functional properties of lysosomal proteases, which are also known as cathepsins, have garnered much interest in recent years due to their therapeutic potential. Studies on the individual cathepsins have uncovered distinct and non-redundant roles for these enzymes. In our laboratory, we have shown that cathepsin L (Ctsl) and cathepsin S (Ctss) are important participants in antigen processing and presentation (1,2). The significant roles of cathepsins have been hypothesized to extend beyond the limits of antigen presentation. As demonstrated in various disease models, cathepsins may also directly process proteins involved in extracellular matrix remodeling, atherosclerosis, cerebral aneurysms, obesity, bone resorption, kidney disease and tumorigenesis (3–9).

In immunity, lysosomal cysteine proteases are involved in MHC class II antigen presentation (10). This is a highly coordinated process involving the proper maturation and trafficking of MHC class II heterodimers, the processing of exogenous antigens, and the loading of peptide antigens onto MHC class II molecules. Exogenous antigens and MHC class II molecules meet in the endosomal compartments. The MHC class II molecule enters the endosomal pathway by its association with the type II membrane glycoprotein, invariant chain (Ii). As a chaperone protein for MHC class II, Ii helps to facilitate its folding in the ER and also targets the Ii/MHCII complex to the endosomes via a signaling motif in its cytoplasmic tail. In the late endosomes, invariant chain is degraded in a sequential manner such that only the Class II-associated Invariant Chain Peptide (CLIP) is left seated in the peptide-binding groove.

In previous work, we showed that the lysosomal cysteine protease Ctsl is abundantly expressed in cortical thymic epithelial cells (cTEC) and that *Ctsl*-deficiency in two haplotypes results in a defect in positive selection specific for CD4+ T cells, suggesting that cTEC in *Ctsl*-deficient mice express an altered peptide repertoire (1). We proposed a novel role for cathepsin L in regulating positive selection by generating the MHC class II bound peptide ligands presented by cTEC. Since then, Maehr et al. (11) reported that *Ctsl*^{-/-} NOD mice are protected from insulinitis and autoimmune diabetes by virtue of a shift in the CD4+ T cell compartment favoring an elevated level of regulatory versus cytotoxic T cells. Overall, Ctsl modulates antigen presentation primarily at the level of cTEC.

On the other hand, Ctss exhibits a different expression pattern than Ctsl, with activity found in dendritic cells, macrophages and B cells (2). Also important for MHC class II maturation in antigen presenting cells, Ctss has been found to influence the presentation of class II-bound epitopes by enhancing or decreasing their presentation. At least in a collagen-induced arthritis model, the absence of Ctss seems to reduce the presentation of type II collagen, thus mitigating the disease (12). Although *Ctsb* does not appear to participate in MHC class II antigen processing and presentation, there is evidence suggesting that it could participate in TNF- α mediated liver injury (13) as well as the onset of pancreatitis (14). Here, we test and compare the roles of all three cathepsin proteins in determining susceptibility to type 1 diabetes mellitus using the NOD mouse.

We have established congenic lines for null alleles of *Ctsl*, *Ctss* and *Ctsb* on the NOD genetic background. We confirmed that *Ctsl*^{-/-} mice are protected from type 1 diabetes (IDDM), and demonstrated a significant reduction in IDDM incidence for *Ctss*^{-/-} and *Ctsb*^{-/-} NOD mice. We confirm that *Ctsl*^{-/-} NOD mice are CD4+ lymphopenic and have an altered ratio of regulatory to activated T cells. We extend previous data by showing that the activated T cells have the same diabetogenic potential as wild-type NOD T cells. Overall, these new congenic strains provide important tools for further studies defining the roles of cathepsin proteases in autoimmunity.

METHODS

Mice

NOD^{scid/scid} were purchased from The Jackson Laboratory (Bar Harbor, ME). NOD mice were originally obtained in 1998 as a kind gift from Charles A. Janeway, Jr. (Department of Immunology, Yale University, New Haven, CT) and have been interbred at the University of Washington through more than 30 generations (NOD/UW). Mice carrying null alleles for *Ctstl*, *Ctss* and *Ctsb* were originally generated using embryonic stem cells derived from a 129/Sv genetic background with implantation into C57BL/6J mice as described for *Ctstl* (15), *Ctss* (16) and *Ctsb* (17). Each allele was introgressed onto the NOD/UW genetic background by successive backcrossing and selection for 19 previously identified *Idd* loci as well as markers at or tightly linked to cathepsins S, L or B (see Supplemental Table 1). The three congenic strains have been fixed to homozygosity for linkage markers at the *Idd* loci and have been maintained by brother-sister mating. All animals were housed in a specific pathogen free animal facility at the University of Washington in a temperature-controlled room (25°C) with a fixed 12-hour light/dark cycle. Mice had free access to food and water. These strains are now under development for distribution at The Jackson Laboratory.

Experimental design

Mice were fed pelleted rodent chow (LabDiet 5053, Teklad, Madison, WI) containing 4% fat (w/w), 24% protein and 4.5% crude fiber. For studies of tissue inflammation, mice were monitored for body weight and urine glucose weekly. Mice exhibiting urine glucose levels (Diastix, Bayer Corp., Elkhart, IL) of greater than 250 mg/dl were deemed diabetic, and this was confirmed by blood glucose measurements (OneTouch Profile, Lifescan, Milpitas, CA). Blood glucose levels of greater than 250 mg/dl were considered diabetic and nearly all mice exhibiting IDDM had blood glucose levels greater than 375 mg/dl. Mice showing no evidence of diabetes by 6 months of age were killed and considered to be non-diabetic. At either IDDM onset or at 6 months of age, mice were killed by cervical dislocation, perfused through the heart apex with sterile PBS, and tissues collected for analyses. Tissues were fixed in 4% buffered formaldehyde and paraffin blocks prepared for sectioning. All procedures were done in accordance with current NIH guidelines and approved by the Animal Care and Use Committee of the University of Washington.

Assessment of insulinitis

Pancreatic tissues were collected, fixed in formalin, sectioned (5 µm thick) and stained with hematoxylin and eosin (H&E). The degree of insulinitis was determined from multiple nonsequential slides from 5 to 6 individual mice (18). Every islet on each section was scored. Each islet was assigned a score, as previously described (19): 0 = no lymphocytic infiltration; 1 = peri-insulinitis; 2 = <50% islet infiltration; and 3 = >50% islet infiltration. An insulinitis score for each mouse was obtained by dividing the total score for each pancreas by the number of islets examined. Data are represented as mean insulinitis score ± SEM for the indicated experimental group.

Assessment of sialadenitis

Submandibular glands from 5 to 6 mice per genotype were collected, fixed in formalin, sectioned (5 µm thick) and H & E stained. The total numbers of lymphocytic foci were counted on each of 3 sections per mouse as described (20). Tissue from the same mice used for insulinitis determination was used for this assessment.

Antibodies

Antibodies against mouse cell surface antigens were purchased from BD Pharmingen: PerCP-conjugated anti-CD4, FITC-conjugated anti-CD8 α , PE-conjugated anti-CD25, APC-conjugated anti-streptavidin. Biotinylated anti-digoxigenin antibody was purchased from Jackson ImmunoResearch Laboratory. Anti-DTA-1 monoclonal antibody, generously provided to us by MJ Turk (Department of Microbiology and Immunology, Dartmouth Medical School, Lebanon NH), was biotinylated in-house and used for the anti-GITR depletion experiments.

Cell isolation and flow cytometry

The cell surface phenotype of thymocyte and lymphocyte populations was determined by four-color flow cytometry. Briefly, thymic, spleen, lymph nodes, and pancreatic lymph nodes were mechanically disrupted. Single cell suspensions were depleted of erythrocytes and approximately 2×10^6 cells were incubated in the presence of fluorescently conjugated antibodies. Binding of biotin-conjugated antibodies was detected by allophycocyanin-conjugated streptavidin. Data was collected using a FACSCalibur™ flow cytometer (Becton Dickinson) and analyzed using FlowJo™ software. Typically, 20,000 events were collected for pancreatic lymph node cell analysis, 50,000 for splenocyte analysis, and 100,000 for thymocyte analysis.

Cell transfer experiments

Erythrocyte-depleted splenocytes from *Ctsl*^{-/-} NOD mice or their wild-type littermate controls were incubated with biotinylated anti-DTA-1 at 5 μ g/ml. GITR-hi cells were selected from the cell suspensions using anti-biotin microbeads and an AutoMACS magnetic cell sorter (Miltenyi, Bergisch Gladbach, Germany). GITR-low or GITR-negative fractions were used for cell transfer experiments. NOD.*scid* mice received 10 – 15×10^6 untouched or GITR-depleted *Ctsl*^{-/-} NOD or wild-type splenocytes by tail-vein injection, and were monitored for the onset of diabetes.

Statistics

Values are reported as means \pm SEM. Statistical differences in diabetes incidence were assessed using the SPSS program (SPSS Inc., Chicago, IL). Groups were compared using Chi-square analyses. In some cases the Student's t-test was used to compare independent means. $P < 0.05$ was accepted as statistically significant.

RESULTS

NOD mice deficient in cathepsin L, but not cathepsin S or B, exhibit complete resistance to diabetes

NOD mice develop spontaneous insulin dependent diabetes mellitus (IDDM) and the incidence and age of onset is influenced by gender and environment (21,22). For female mice, onset occurs at approximately four to six months of age and incidence ranges between 60%–100% depending upon the colony. Diabetes develops at a slower rate in males, which tend to exhibit more resistance to the disease. Because females are more susceptible to diabetes than males, we used females to assess diabetes incidence among our strains.

With the exception of *Ctsl*^{-/-} mice, all cathepsin deficient strains developed diabetes to some extent (Figure 1). *Ctss*^{+/-} matched the IDDM incidence as seen for NOD (69%), and *Ctsb*^{+/-} and *Ctsl*^{+/-} showed modest but significantly reduced values as compared with NOD mice (50% [$p=0.0061$] and 55% [$p=0.035$], respectively) (Figure 1A). For homozygous null cathepsin S and B congenic mice, diabetes occurred at significantly lower incidences as

compared to their heterozygous littermates and NOD ($p < 0.00001$ versus NOD and littermates). Cathepsin-deficient mice developed diabetes between 4.5 – 5.5 months of age which was later than seen for NOD (3.9 months; $p < 0.00001$) (Figure 1B). Incidence curves for homozygous (Figure 1C) and heterozygous (Figure 1D) null mice are also shown to directly contrast the strains.

Ctsl^{-/-} NOD mice exhibited a dramatic phenotype, marked by complete resistance to diabetes. As the absence of diabetes could be due to retarded kinetics of the disease, *Ctsl*^{-/-} mice were maintained and monitored over a longer period of time. Mice that were allowed to age up to ten months of age never developed diabetes, indicating that our failure to observe diabetes in these mice was not due to delayed kinetics.

Insulinitis and peripheral lymphocytic infiltration occurs in NOD mice deficient in cathepsin B or S

Type 1 diabetes mellitus in humans and NOD mice is characterized by progressive stages of lymphocytic infiltration of pancreatic islets, eventually resulting in islet destruction and the onset of IDDM (23). However, infiltration of pancreatic islets does not necessarily result in islet cell pathology and loss of islet cell function as has been observed in a closely related strain, NOR (24). Therefore, we sought to determine whether we could detect the presence of mononuclear cell infiltrates in the pancreatic tissues of cathepsin-deficient NOD mice.

Histological analysis of pancreatic sections revealed that overall, diabetic cathepsin deficient mice had insulinitis scores comparable to that of the diabetic NOD parental strain (Figure 2A), although values were significantly reduced for homozygous cathepsin S and B-deficient mice ($p < 0.03$ versus NOD). Nondiabetic mice also showed measurable insulinitis which was significantly reduced as compared to their diabetic counterparts ($p < 0.00001$ to $p < 0.025$ [Figure 2A]). *Ctsl*-deficient congenic mice were set apart from the other strains in that insulinitis was absent in non-diabetic animals (Figure 2A, B).

To test whether cathepsin deficiency influenced autoimmune responses at additional tissue sites as seen for NOD (20), we scored salivary gland tissues for sialadenitis in homozygous cathepsin deficient genotypes at 6 months of age. Sialadenitis was noted in both diabetic and non-diabetic mice (Figure 2C), the extent of which was comparable between NOD and cathepsin S and B strains (12–20 lesions per mouse). Values tended to be lower (~6.5 lesions/mouse) for nondiabetic *Ctsl*^{-/-} mice. Overall, cathepsin deficient mice experience peripheral infiltration.

The reduced insulinitis observed in each homozygous cathepsin-deficient group (Figure 2A) led us to examine whether the pancreata of these mice could possibly be resistant to infiltration. It has been suggested that cathepsins are involved in extracellular matrix remodeling, and thereby can potentially influence the accessibility of the pancreas to autoreactive islet-specific T cells (25–27). To determine if this was the case, we assessed the ability of T cell receptor transgenic T cells of known reactivity to beta-islet cell antigens to induce diabetes in the cathepsin-deficient NOD mice. Activated CD8⁺ and CD4⁺ diabetogenic T cell clones (2×10^6 insulin-reactive G9C8 or 10×10^6 GAD65-specific BDC2.5, respectively) (28,29) were transferred into sublethally irradiated *Ctss*^{-/-}, *Ctsb*^{-/-} and *Ctsl*^{-/-} NOD mice, and blood glucose levels in these mice were monitored. Mice in each group developed diabetes with similar kinetics within 4–6 days after transfer (data not shown), implying that the pancreatic tissues in these mice are not necessarily resilient to infiltration and destruction by pathogenic T cells. This experiment also indicates that presentation of specific beta-islet cell antigens occurs in all three cathepsin deficient mice, and is sufficient to induce diabetes.

Cathepsin L-deficient NOD mice exhibit a defect in CD4⁺ T cell selection and an increase in the relative size of the Foxp3⁺ regulatory T cell subset

It is known that cathepsin L deficiency causes a profound defect in CD4⁺ T cell development which is MHC class II haplotype independent (1,11). In addition, for another colony of *Ctsl*^{-/-} NOD mice (11), disease resistance was shown to be associated with both the smaller CD4⁺ T cell population, a reduced CD4:CD8 ratio and an increased ratio of regulatory CD4⁺ T cells as compared to normal CD4⁺ T cells. We confirmed these findings in our new colony of *Ctsl*^{-/-} NOD mice. We found that CD4⁺ T cells were 3-fold reduced in thymus and lymph nodes of *Ctsl*-deficient versus *Ctsl*-sufficient NOD mice (Figure 3A). We also showed that the reduced CD4:CD8 ratio offered protection from diabetes by looking for diabetes development in lymphopenic NOD (NOD.*scid*) mice that received 15×10⁶ splenocytes from pre-diabetic *Ctsl*-heterozygote NOD mice. The CD4:CD8 ratio of the *Ctsl*-heterozygote NOD splenocytes was adjusted to resemble that seen in *Ctsl*^{-/-} NOD mice (Figure 3A) by the addition of CD8⁺ T cells isolated from *Catl*-heterozygote NOD mice. NOD.*scid* recipients of *Ctsl*-sufficient or *Ctsl*-deficient NOD splenocytes were then monitored for hyperglycemia. Up to 75 days post-transfer, neither group developed diabetes. This result raised the possibility that a skewed CD4:CD8 ratio is responsible for protection against diabetes. However, flow cytometric analysis revealed that CD4:CD8 ratios in both groups had approached a ratio normally seen in wild-type mice (Figure 3B) showing that diabetes was not dependent upon a skewed CD4:CD8 ratio. Upon further examination using flow cytometry, we found an enrichment in Foxp3-expressing cells in splenocytes in recipients of T cells from *Ctsl*-heterozygote and *Ctsl*^{-/-} NOD mice (Figure 3C). These results suggested that an expanded regulatory T cell population prevented diabetes progression in both groups.

Consistent with the hypothesis that the regulatory T (Tr) cell population is offering protection against diabetes in *Ctsl*^{-/-} NOD mice, we found a 2-fold higher frequency of Foxp3-expressing CD4⁺ T cells in unmanipulated *Ctsl*^{-/-} NOD mice compared to heterozygote controls (Figure 4). We also observed an increased proportion of Foxp3-expressing T cells in *Catl*-deficient C57BL/6 mice, leading us to believe that the increase in the proportion of Tr cells in the absence of Cathepsin L is not a strain-dependent phenomenon (data not shown). Therefore, in an autoimmune disease-susceptible strain, it is highly likely that an imbalance in the proportion of regulatory to autoreactive effector T cells, in favor of regulatory T cells, led to a completely penetrant form of protection against disease development.

Diabetogenic T cells develop in *Cathepsin L*-deficient NOD mice

Islet-reactive T cells were shown to exist in mice of the *Ctsl*^{-/-} NOD colony established by Maehr et al. (11). Here we confirm this occurs in our colony and show the extent of diabetogenic potential of these cells. To determine whether pathogenic T cells develop in our *Ctsl*^{-/-} NOD mice, we examined the pathogenic potential of their splenocytes. Because we observe an enrichment of Tr cells in *Ctsl*^{-/-} NOD mice, and our previous experiments in NOD.SCID mice also suggest that the presence of Tr cells may delay the onset of diabetes, we wanted to determine whether Tr-depleted splenocytes from *Ctsl*^{-/-} NOD mice could induce diabetes. Using GITR antibody-mediated MACS depletion, we depleted GITR^{hi} T cells from splenocytes before transferring them into NOD.*scid* mice (Figure 5A). GITR, a member of the tumor necrosis receptor family, is highly expressed on Tr cells and its expression – in comparison to CD25 – correlates better with Foxp3 expression (30). 10–15×10⁶ GITR-depleted or control splenocytes from 8–9 week-old *Ctsl*-heterozygous NOD or *Ctsl*^{-/-} NOD mice were then adoptively transferred into 5–6 week-old NOD.*scid* hosts. The incidence of diabetes in each group was determined over the course of 11 weeks. Recipients of control splenocytes from *Ctsl*-heterozygous NOD mice had a diabetes incidence of 23.07 %, while none of the recipients of control *Ctsl*^{-/-} NOD splenocytes developed diabetes (Figure 5B). However, recipients of GITR-depleted splenocytes from *Ctsl*-heterozygous NOD and *Ctsl*^{-/-} NOD mice

developed diabetes at a similar rate and frequency (41.7% and 45.5%, respectively) (Figure 5B). These data show that diabetogenic T cells develop in *Ctstl*^{-/-} NOD mice, and suggest that splenocytes from these mice are just as capable of inducing diabetes as splenocytes from *Ctstl*-heterozygous NOD mice.

Through these adoptive cell transfer studies in NOD.SCID mice, we also rule out effects of the lack of *Ctstl* expression on non-hematopoietic cells, a finding consistent with that of Maehr et al. (11). Together, our results suggest that the presence of an expanded Tr cell population in *Ctstl*^{-/-} NOD mice prevents the activation of diabetogenic T cells and mononuclear cell infiltration of beta-islet cells.

DISCUSSION

We have shown that in a spontaneous model of autoimmune diabetes, deficiency in Cathepsin S, Cathepsin B, or Cathepsin L offers protection from type I diabetes mellitus development on the NOD background. Deficiency in Cathepsin S or Cathepsin B led to a decrease in diabetes incidence, whereas deficiency in Cathepsin L provided complete resistance to the disease.

Incomplete penetrance in *Ctstl*^{-/-} or *Ctstb*^{-/-} NOD mice is surprising given the important roles of Cathepsin S and B in antigen processing and presentation by MHC class II molecules to CD4 cells. At this point it is not known if incomplete penetrance is due to reduced generation of autoreactive T cells or to other non-specific inflammatory activities initiated or perpetuated by these enzymes. The reduced penetrance could be attributed to their ascribed functions outside of MHC class II antigen processing and presentation. Some support for this idea is provided by the observation that in NOD splenocytes, Ctss is not required for removal of Ii remnants from class II MHC molecules, as demonstrated using a Ctss-specific inhibitor (11). Additionally, Ctss has been recently shown to participate in leukocyte infiltration, medial elastic lamina degradation, endothelial cell invasion, and neovascularization in atherosclerosis-prone mice (31). Ctstb may contribute to the autoimmune processes through pathways involving inflammation and apoptosis. The absence of Ctstb results in decreased liver injury as a result of mitigated TNF alpha-induced apoptosis (13). Ctstb has also been shown to participate in the export of TNFalpha from macrophages (32). In addition, Ctstb regulates matrix degradation and the invasiveness of human glioblastoma cell lines, and therefore could also regulate the accessibility of autoreactive T cells to the pancreas (33). Because even diabetic *Ctss*- or *Ctstb*-deficient NOD mice displayed decreased peri-insulinitis and islet cell infiltration, it is possible that pathogenic T cells were not optimally activated to program tissue infiltration. It is possible that if *Ctss*- and *Ctstb*-deficient mice were allowed to age beyond six months of age, diabetes incidence would increase. Some evidence for this is suggested by the similarity in insulinitis score between diabetic and non-diabetic *Ctstb* heterozygous mice (Figure 2). As more autoreactive T cells are activated by the increased presentation of pancreatic antigens and the threshold for autoreactivity is reached, diabetes would likely ensue.

Unlike *Ctss*- or *Ctstb*-deficient NOD mice, *Ctstl*-deficient NOD mice exhibit complete disease resistance. We have ruled out the possibility that diabetogenic T cells do not develop in *Ctstl* deficient mice, because Tr cell-depleted splenocytes from *Ctstl*-deficient NOD mice were equally capable of inducing diabetes in NOD.SCID mice, compared to splenocytes from *Ctstl*-sufficient NOD mice. These findings are different from those of Maehr et al., who also examined the phenotype of *Ctstl*-deficiency in NOD mice and found that the pathogenicity of splenocytes from *Ctstl*-deficient NOD mice was reduced (11). We also found that *Ctstl*-deficient NOD mice were not more resistant to T cell-dependent tissue damage, as transferred diabetogenic T cell clones were perfectly capable of inducing disease in these mice. Instead, an increase in the frequency of Tr cells appears to be primarily responsible for disease resistance. Earlier studies by Salomon et al. demonstrated that the transfer of Tr cells inhibits

the progression of diabetes in NOD mice lacking Tr cells (34). In contrast to observations by Chen and colleagues (35), we find that protection mediated by Tr cells may also occur prior to islet infiltration – not only in the pancreatic tissue itself – as suggested by the complete lack of islet cell infiltration observed in *Ctsl*-deficient NOD mice.

While our studies provided a likely explanation for disease resistance in *Ctsl*-deficient NOD mice, the roles of *Ctsb* and *Ctss* in autoimmune diabetes deserve further examination. Manipulation of Cathepsin activity may offer new insights to clinical applications in autoimmune diabetes as well as other autoimmune diseases.

Supplementary Material

Refer to Web version on PubMed Central for supplementary material.

Acknowledgments

This work was supported by grants from NIH (RO1 DK063159 [RCL] and AI34206 [AYR] and a Pilot and Feasibility grant awarded by the Diabetes Endocrinology Research Center (NIH P30 DK017047) [AYR]). We would like to acknowledge Dr. Alexander Chervonsky (Department of Pathology, University of Chicago, Chicago, IL) for help with data collection and review of study proposal.

REFERENCES

1. Honey K, Rudensky AY. Lysosomal cysteine proteases regulate antigen presentation. *Nat Rev Immunol* 2003;3:472–482. [PubMed: 12776207]
2. Beers C, Burich A, Kleijmeer MJ, Griffith JM, Wong P, Rudensky AY. Cathepsin S controls MHC class II-mediated antigen presentation by epithelial cells in vivo. *J Immunology* 2005;174:1205–1212. [PubMed: 15661874]
3. Aoki T, Kataoka H, Ishibashi R, Nozaki K, Hashimoto N. Cathepsin B, K, and S are expressed in cerebral aneurysms and promote the progression of cerebral aneurysms. *Stroke* 2008;39:603–2610.
4. Sukhova GK, Zhang Y, Pan JH, Wada Y, Yamamoto T, Naito M, Kodama T, Tsimikas S, Witztum JL, Lu ML, Sakara Y, Chin MT, Libby P, Shi GP. Deficiency of cathepsin S reduced atherosclerosis in LDL receptor-deficient mice. *J Clin Invest* 2003;111:897–906. [PubMed: 12639996]
5. Burden RE, Snoddy P, Buick RJ, Johnston JA, Walker B, Scott CJ. Recombinant cathepsin S propeptide attenuates cell invasion by inhibition of cathepsin L-like proteases in tumor microenvironment. *Mol Cancer Ther* 2008;7:538–547. [PubMed: 18347141]
6. Sever S, Altintas MM, Nankoe SR, Möller CC, Ko D, Wei C, Henderson J, de Re EC, Hsing L, Erickson A, Cohen CD, Kretzler M, Kerjaschki D, Rudensky A, Nikolic B, Reiser J. Proteolytic processing of dynamin by cytoplasmic cathepsin L is a mechanism for proteinuric kidney disease. *J Clin Invest* 2007;117:2095–2104. [PubMed: 17671649]
7. Kitamoto S, Sukhova GK, Sun J, Yang M, Libby P, Love V, Duramad P, Sun C, Zhang Y, Yang X, Peters C, Shi GP. Cathepsin L deficiency reduces diet-induced atherosclerosis in low-density lipoprotein receptor-knockout mice. *Circulation* 2007;115:2065–2075. [PubMed: 17404153]
8. Baici A, Lang A, Zwicky R, Müntener K. Cathepsin B in osteoarthritis:uncontrolled proteolysis in the wrong place. *Semin Arthritis Rheum* 2005;34:24–28. [PubMed: 16206953]
9. Taleb S, Clément K. Emerging role of cathepsin S in obesity and its associated diseases. *Clin Chem Lab Med* 2007;45:328–332. [PubMed: 17378727]
10. Hsing LC, Rudensky AY. The lysosomal cysteine proteases in MHC class II antigen presentation. *Immunol Rev* 2005;207:229–241. [PubMed: 16181340]
11. Maehr R, Mintern JD, Herman AE, Lennon-Duménil A-M, Mathis D, Benoist C, Ploegh HL. Cathepsin L is essential for onset of autoimmune diabetes in NOD mice. *J Clin Invest* 2005;115:2934–2943. [PubMed: 16184198]
12. Nakagawa TY, Brissette WH, Lira PD, Griffiths RJ, Petrushova N, Stock J, McNeish JD, Eastman SE, Howard ED, Clarke SR, Rosloniec EF, Elliott EA, Rudensky AY. Impaired invariant chain

- degradation and antigen presentation and diminished collagen-induced arthritis in cathepsin S null mice. *Immunity* 1999;10:207–217. [PubMed: 10072073]
13. Guicciardi ME, Deussing J, Miyoshi H, Bronk SF, Svingen PA, Peters C, Kaufmann SH, Gores GJ. Cathepsin B contributes to TNF- α -mediated hepatocytes apoptosis by promoting mitochondrial release of cytochrome c. *J Clin Invest* 2000;106:1127–1137. [PubMed: 11067865]
 14. Halangk W, Lerch MM, Brandt-Nedelev B, Roth W, Ruthenbuerger M, Reinheckel T, Domschke W, Lippert H, Peters C, Deussing J. Role of cathepsin B in intracellular trypsinogen activation and the onset of acute pancreatitis. *J Clin Invest* 2000;106:773–781. [PubMed: 10995788]
 15. Roth W, Deussing J, Botchkarev VA, Pauly-Evers M, Saftig P, Hafner A, Schmidt P, Schmahl W, Scherer J, Anton-Lamprecht I, Von Figura K, Paus R, Peters C. Cathepsin L deficiency as molecular defect of furless: hyperproliferation of keratinocytes and perturbation of hair follicle cycling. *FASEB J* 2000;14:2075–2086. [PubMed: 11023992]
 16. Shi G-P, Villadangos JA, Dranoff G, Small C, Gu L, Haley KJ, Riese R, Ploegh HL, Chapman HA. Cathepsin S required for normal MHC Class II peptide loading and germinal center development. *Immunity* 1999;10:197–206. [PubMed: 10072072]
 17. Halangk W, Lerch MM, Brandt-Nedelev B, Roth W, Rughenbuerger M, Reinheckel T, Domschke W, Lippert H, Peters C, Deussing J. Role of cathepsin B in intracellular trypsinogen activation and the onset of acute pancreatitis. *J Clin Invest* 2000;106:773–781. [PubMed: 10995788]
 18. Deeg MA, Bowen RF, Williams MD, Olson LK, Kirk EA, LeBoeuf RC. Increased expression of GPI-specific phospholipase D in mouse models of type 1 diabetes. *Am J Physiol Endocrinol Metab* 2001;281:E147–E154. [PubMed: 11404232]
 19. Debussche X, Lormeau B, Boitard C, Toub Blanc M, Assan R. Course of pancreatic beta cell destruction in prediabetic NOD mice: a histomorphometric evaluation. *Diabetes Metab* 1994;20:282–290.
 20. Yamano S, Atkinson JC, Baum BJ, Fox PC. Salivary gland cytokine expression in NOD and normal BALB/c mice. *Clin Immunol* 1999;92:265–275. [PubMed: 10479531]
 21. Serreze DV, Leiter EH. Genetic and pathogenic basis of autoimmune diabetes in NOD mice. *Curr Opin Immunol* 1994;6:900–906. [PubMed: 7710714]
 22. Leiter EH, Serreze DV. Antigen presenting cells and the immunogenetics of autoimmune diabetes in NOD mice. *Reg Immunol* 1992;4:263–273. [PubMed: 1290746]
 23. Yoon J-W, Jun H-S. Autoimmune destruction of pancreatic β cells. *Amer J Therap* 2005;12:580–591. [PubMed: 16280652]
 24. Prochazka M, Serreze DV, Frankel WN, Leiter EH. NOR/Lt mice: MHC-matched diabetes-resistant control strain for NOD mice. *Diabetes* 1992;41:98–106. [PubMed: 1727742]
 25. Lakka SS, Gondi CS, Yanamandra N, Olivero WC, Dinh DH, Gujrati M, Rao JS. Inhibition of cathepsin B and MMP-9 gene expression in glioblastoma cell line via RNA interference reduces tumor cell invasion, tumor growth and angiogenesis. *Oncogene* 2004;23:4681–4689. [PubMed: 15122332]
 26. Liu J, Sukhova GK, Sun JS, Xu WH, Libby P, Shi GP. Lysosomal cysteine proteases in atherosclerosis. *Arterioscler Thromb Vasc Biol* 2004;24:1359–1366. [PubMed: 15178558]
 27. Woods CC, Sundar K, Tessler C, Lebsack TW, Grainger L, Nielsen A, Bleich D, DeLuca D. Tissue inhibitor of metalloproteinase-2 inhibits T-cell infiltration and preserves pancreatic beta-cell function in an in vitro type 1 diabetes mellitus model. *J Autoimmun* 2006;27:28–37. [PubMed: 16765565]
 28. Katz JD, Wang B, Haskins K, Benoist C, Mathis D. Following a diabetogenic T cell from genesis through pathogenesis. *Cell* 1993;74:1089–1100. [PubMed: 8402882]
 29. Wong FS, Karttunen J, Dumont C, Wen L, Visintin I, Pilip IM, Shastri N, Pamer EG, Janeway CA Jr. Identification of an MHC class I-restricted autoantigen in type 1 diabetes by screening an organ-specific cDNA library. *Nat Med* 1999;5:1026–1031. [PubMed: 10470079]
 30. Ono M, Shimizu J, Miyachi Y, Sakaguchi S. Control of autoimmune myocarditis and multiorgan inflammation by glucocorticoid-induced TNF receptor family-related protein(high), Foxp3-expressing CD25+ and CD25- regulatory T cells. *J Immunol* 2006;176:4748–4756. [PubMed: 16585568]
 31. Liu J, Sukhova GK, Sun JS, Xu WH, Libby P, Shi GP. Lysosomal cysteine proteases in atherosclerosis. *Arterioscler Thromb Vasc Biol* 2004;24:1359–1366. [PubMed: 15178558]

33. Woods CC, Sundar K, Tessler C, Lebsack TW, Grainger L, Nielsen A, Bleich D, DeLuca D. Tissue inhibitor of metalloproteinase-2 inhibits T-cell infiltration and preserves pancreatic beta-cell function in an in vitro type 1 diabetes mellitus model. *J Autoimmun* 2006;27:28–37. [PubMed: 16765565]
34. Salomon B, Lenschow DJ, Rhee L, Ashourian N, Singh B, Sharpe A, Bluestone JA. B7/CD28 costimulation is essential for the homeostasis of the CD4+CD25+ immunoregulatory T cells that control autoimmune diabetes. *Immunity* 2000;12:431–440. [PubMed: 10795741]
35. Chen Z, Herman AE, Matos M, Mathis D, Benoist C. Where CD4+CD25+ T reg cells impinge on autoimmune diabetes. *J Exp Med* 2005;202:1387–1397. [PubMed: 16301745]

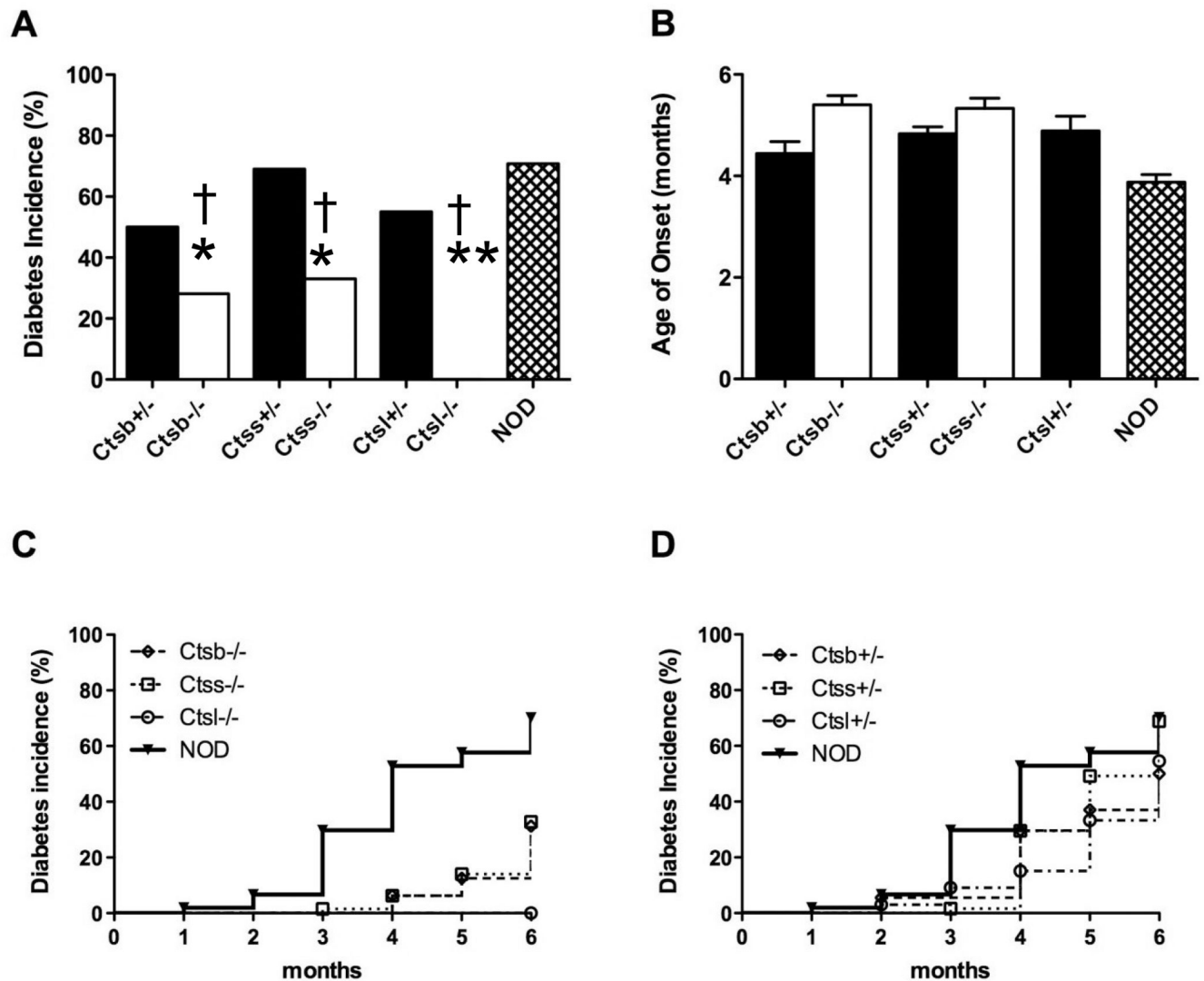


Figure 1. Cathepsin-deficient NOD mice exhibit resistance to spontaneous autoimmune diabetes mellitus

Female cathepsin-deficient mice and their heterozygous littermate controls were monitored for diabetes and were sacrificed upon diagnosis with diabetes or at six months of age as described in Materials and Methods. **(A)** Diabetes incidence of cathepsin L (Ctsl), cathepsin S (Ctss)- and cathepsin B (Ctsb)-deficient mice (heterozygous, filled bars; homozygous, open bars).

(B) Mean age of onset for cathepsin-deficient mice. Homozygous *Catl*^{-/-} mice are completely protected from diabetes with remaining strains showing age of onset between 4 to 6 months.

(C) Kaplan-Meier curves for diabetes incidence for NOD (filled circles) and homozygous cathepsin-deficient strains. *Ctsl*^{-/-} (filled diamonds) are completely protected from diabetes onset. *Ctss*^{-/-} (filled squares) and *Ctsb*^{-/-} (filled triangles) show reduced onset levels (33% and 25%, respectively) as compared to wild-type NOD (69%).

(D) Kaplan-Meier curves for diabetes incidence among cathepsin-heterozygous mice. *Ctss*^{+/-} (open squares) show incidence as for the NOD strain (69%), while *Ctsb*^{+/-} (open triangles) and *Ctsl*^{+/-} (open diamonds) have somewhat reduced diabetes incidence (50% and 55%, respectively).

Numbers of cohorts per group monitored were (cathepsin-deficient; cathepsin-heterozygous littermate controls): *Ctsl*: 25;32, *Ctss*: 43;54, *Ctsb*: 60;47 and NOD: 105. **P*<0.05,

** $p < 0.00001$ between NOD and cathepsin-deficient genotypes; † $p < 0.00001$ between diabetic and non-diabetic mice within genotype. Data are presented as mean \pm SEM.

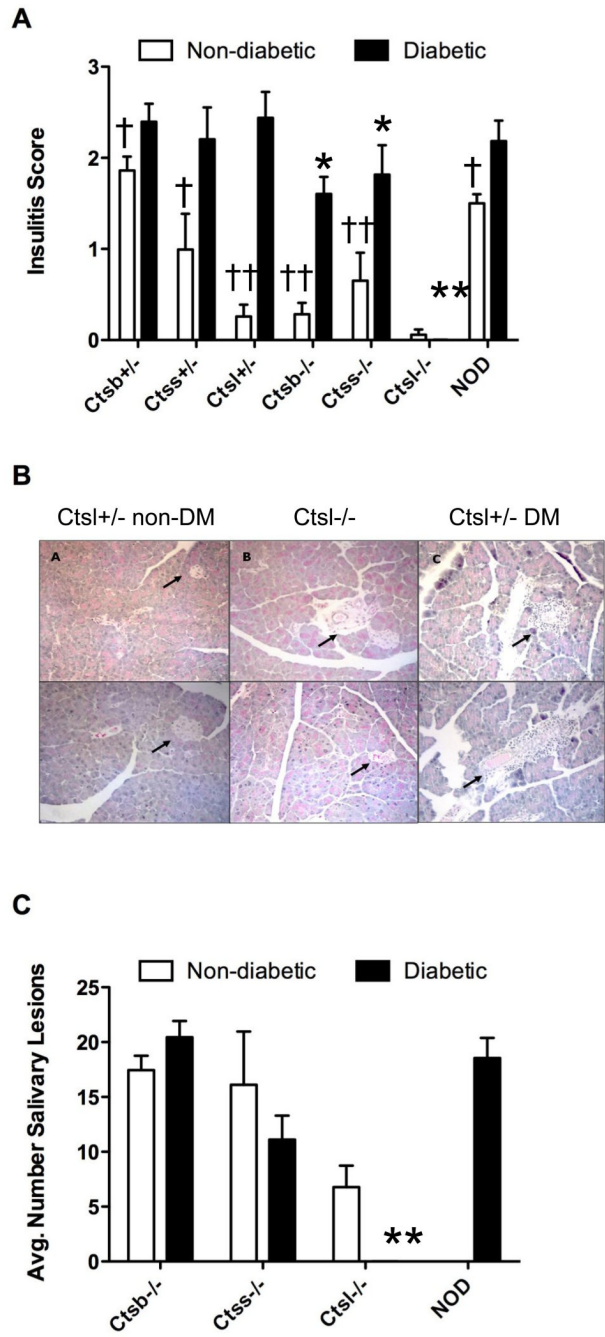


Figure 2. Insulinitis and sialadenitis among cathepsin-deficient NOD mice

Five to 6 mice from each genotype were analyzed for lymphocytic infiltration by histological analyses as described in Materials and Methods. (A) Insulinitis is markedly reduced in *Catsl*^{-/-} NOD mice. Pancreata were harvested from mice and fixed in 10% formalin. Pancreatic tissue sections were processed for hematoxylin and eosin (H&E) staining to assess mononuclear cell infiltration. Pancreatic sections were graded for insulinitis, based on a scale from 0 to 3; 0=no insulinitis, 1=peri-insulinitis, 2 =<50% infiltration, 3 =>50% infiltration. (B) Pancreatic sections from nondiabetic (non-DM) cathepsin L-sufficient, cathepsin L-sufficient and control diabetic (DM) *Catsl*^{+/-} NOD mice demonstrating insulinitis only in the control strain. (C) Sialadenitis is comparable among diabetic and nondiabetic cathepsin-deficient and NOD strains.

Inflammation tended to be reduced in *Ctsl*^{-/-} nondiabetic mice but differences from NOD did not reach significance. *P<0.03 and **p<0.00001 between diabetic NOD and diabetic cathepsin-deficient strains, n=5–6 mice per genotype. †P<0.03 and ††p<0.00001 within genotype between non-diabetic and diabetic mice. Data are presented as mean ± SEM.

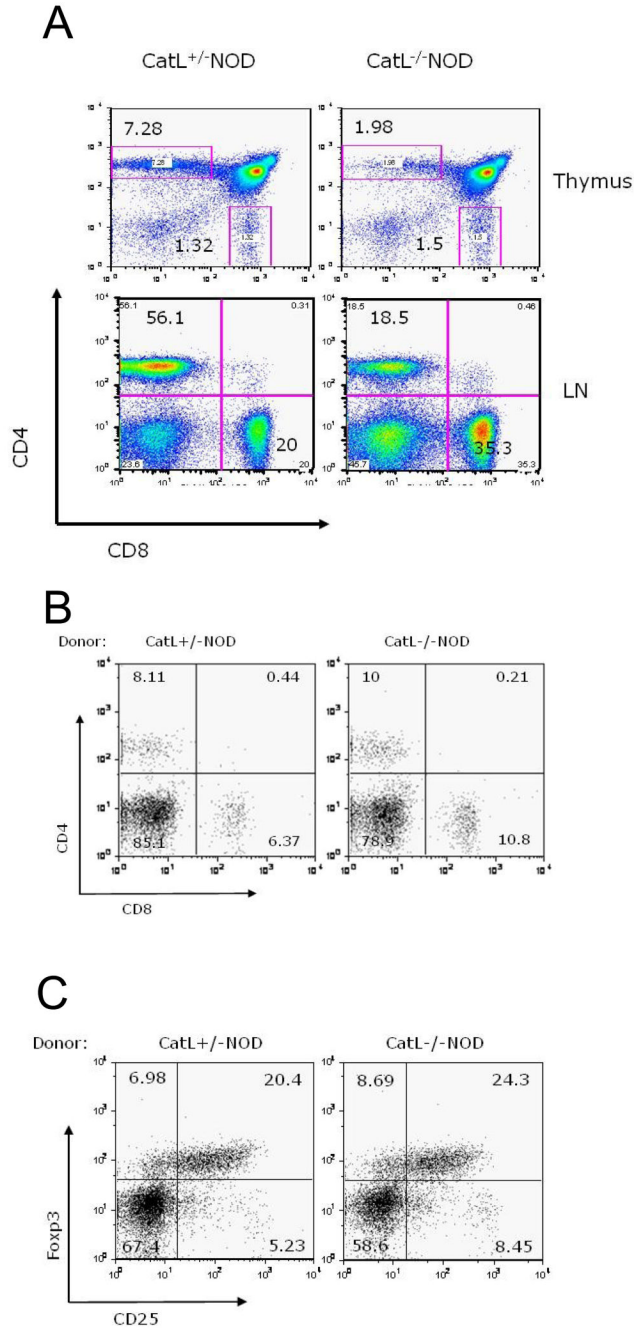


Figure 3. Characterization of T-cells in cathepsin L-deficient (*Ctsl*^{-/-}) mice

(A) *Ctsl*^{-/-} NOD mice exhibit a defect in CD4⁺ T-cell selection as seen by comparing ratios of CD4/CD8 in the thymus and lymph nodes of *Ctsl*-sufficient and *Ctsl*-deficient NOD mice. Thymocytes and lymphocytes from *CatL*^{+/-} and *CatL*^{-/-} mice were stained with PerCP conjugated anti-CD4 and APC-conjugated anti-CD8 antibodies (BD Pharmingen), and CD4/CD8 ratios were determined using flow cytometry. (B) CD4:CD8 ratio is adjusted in *Ctsl*^{-/-} congenic splenocytes to resemble that of *Ctsl*^{+/-} splenocytes for the adoptive transfer study. Peripheral blood was taken from NOD.*scid* recipients for flow cytometry 48 days after the splenocytes were transferred into NOD.*scid* recipients. (C) Lymphopenic conditions in NOD.*scid* hosts induce Foxp3⁺ regulatory T cell expansion, regardless of the genotype of the

donor cells. We show Foxp3 profiles of splenocytes from NOD.*scid* recipients 75 days post-transfer. Cells were gated on the CD4+ T cell population. N=11–13 in each group and representative scans are shown here.

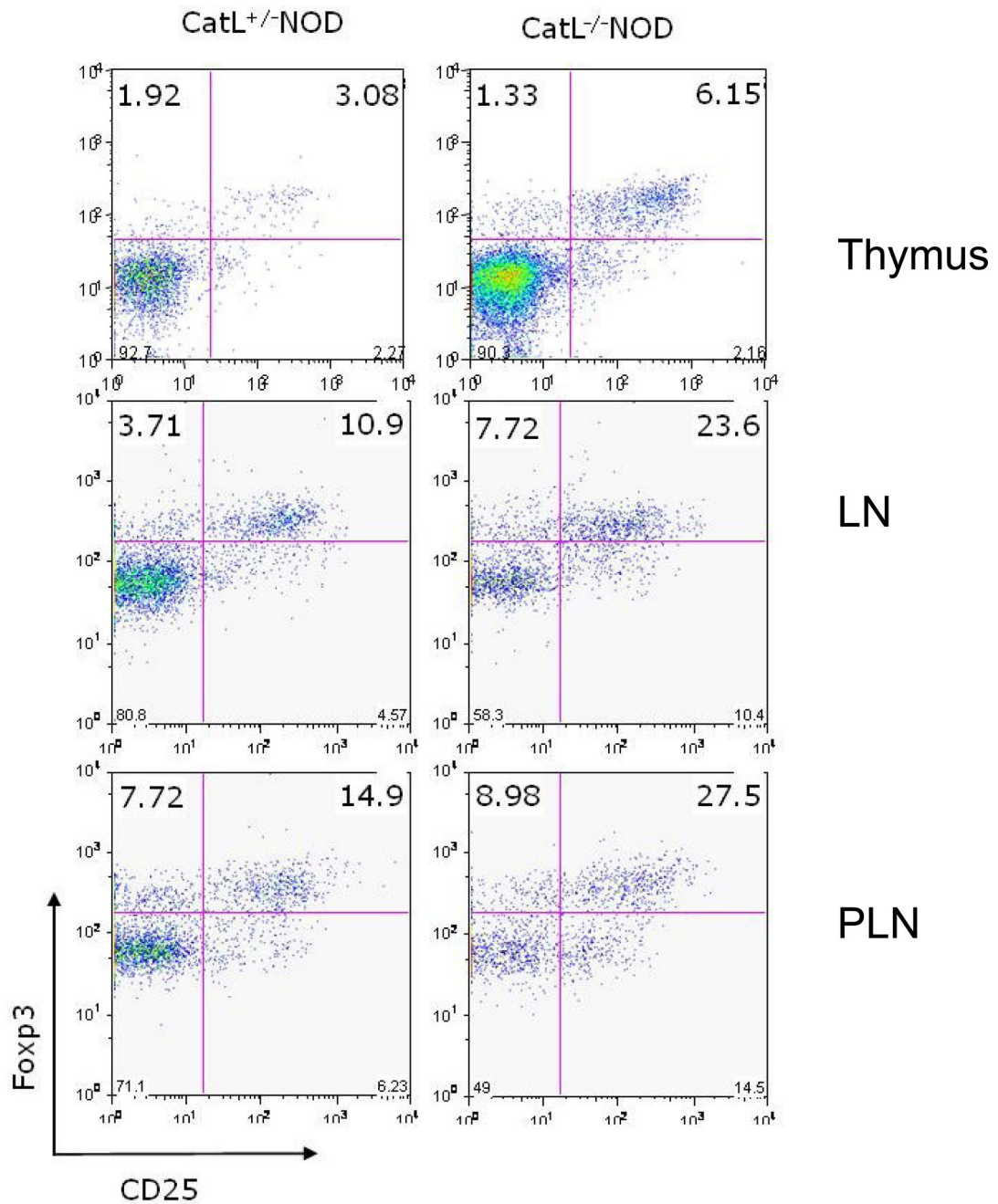


Figure 4. Foxp3⁺ regulatory T-cells are present at a higher proportion in *Ctsl*^{-/-} NOD mice in comparison to littermate controls

Foxp3 profiles of lymphocytes from thymus, lymph nodes (LN), and pancreatic lymph nodes (PLN) from 6 month-old *Ctsl*-sufficient and *Ctsl*-deficient NOD mice. Cells were gated on the CD4⁺ T cell population. Regulatory T cell frequency was assessed using a rabbit polyclonal antibody against Foxp3. N=11–13 in each group and representative scans are shown here.

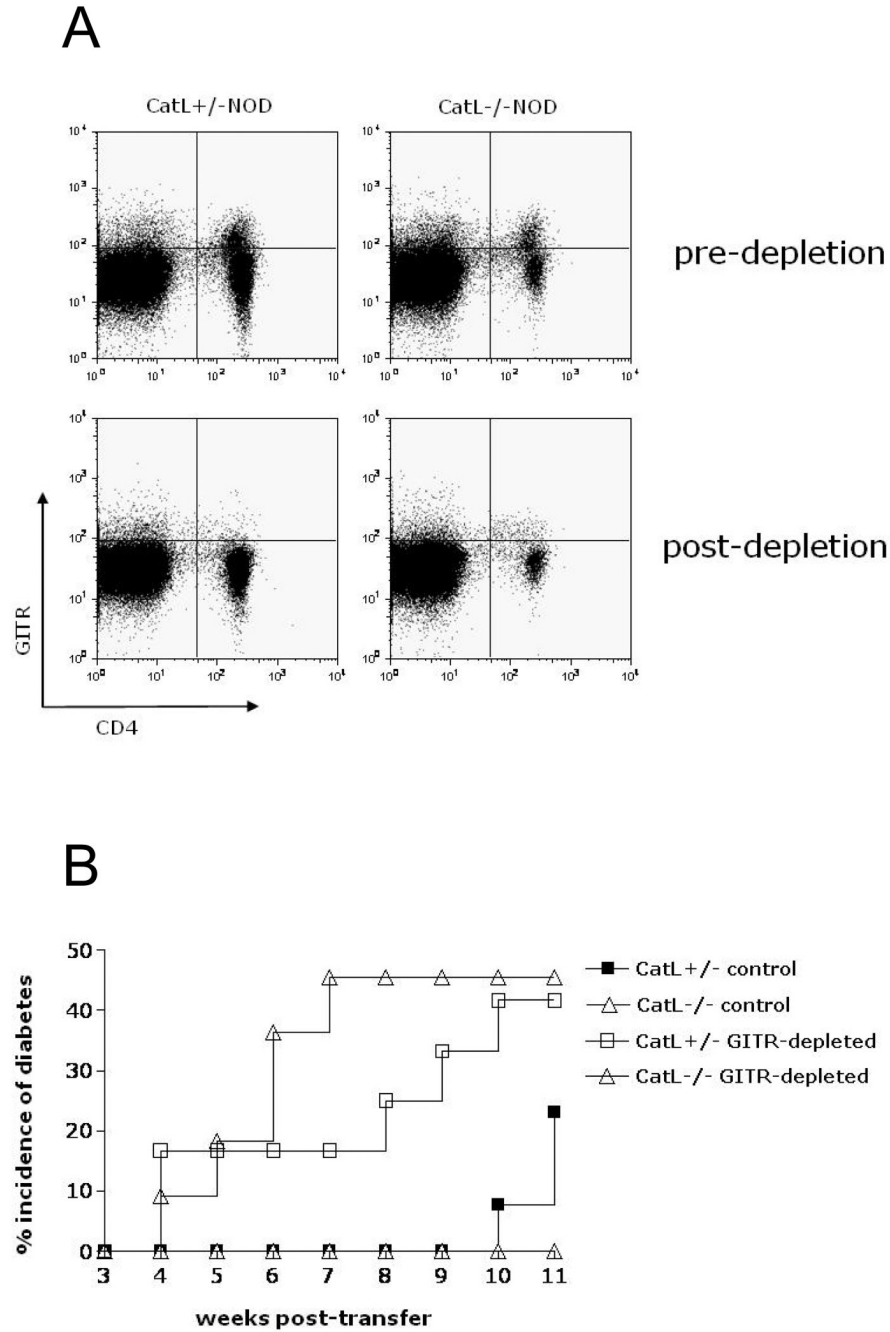


Figure 5. Anti-GITR depletion of splenocytes from *CtSL*-sufficient and *CtSL*-deficient NOD mice (A) Depletion with DTA-1 monoclonal antibody results in the exclusion of $GITR^{hi}$ cells, but not $GITR^{lo}$ cells. (B) Diabetogenic T-cells develop in *CtSL*^{-/-} NOD mice and are pathogenic. Transfer of GTR-depleted splenocytes from *CtSL*-deficient and *CtSL*-sufficient mice induced diabetes in NOD.*scid* mice with similar kinetics. NOD.*scid* recipient mice received $10\text{--}15 \times 10^6$ GTR-depleted or control splenocytes from *CtSL*-deficient and *CtSL*-sufficient mice by i.v. injection and their blood glucose levels were monitored for 11 weeks. There were n=11–13 mice in each group; $p < 0.00001$ between control and GTR-depleted groups through 10 weeks post-transfer; $p < 0.001$ between *CatL* heterozygous and homozygous groups between 7 to 9 weeks post transfer.